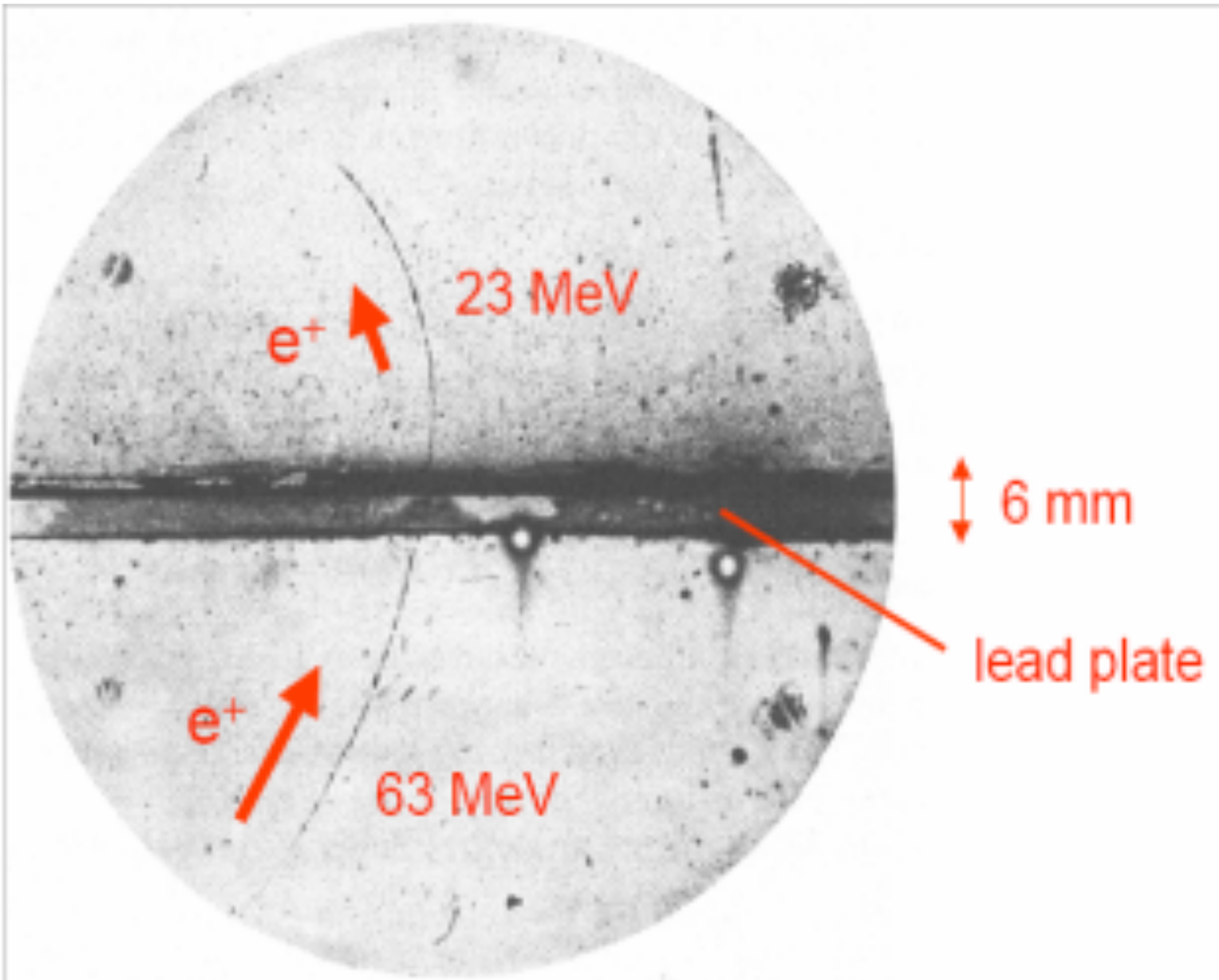

Esperimento di Anderson (1933)
Camera a nebbia costruita con Millikan
in campo magnetico da 15kG

Phys. Rev. 142, 3 (1965)

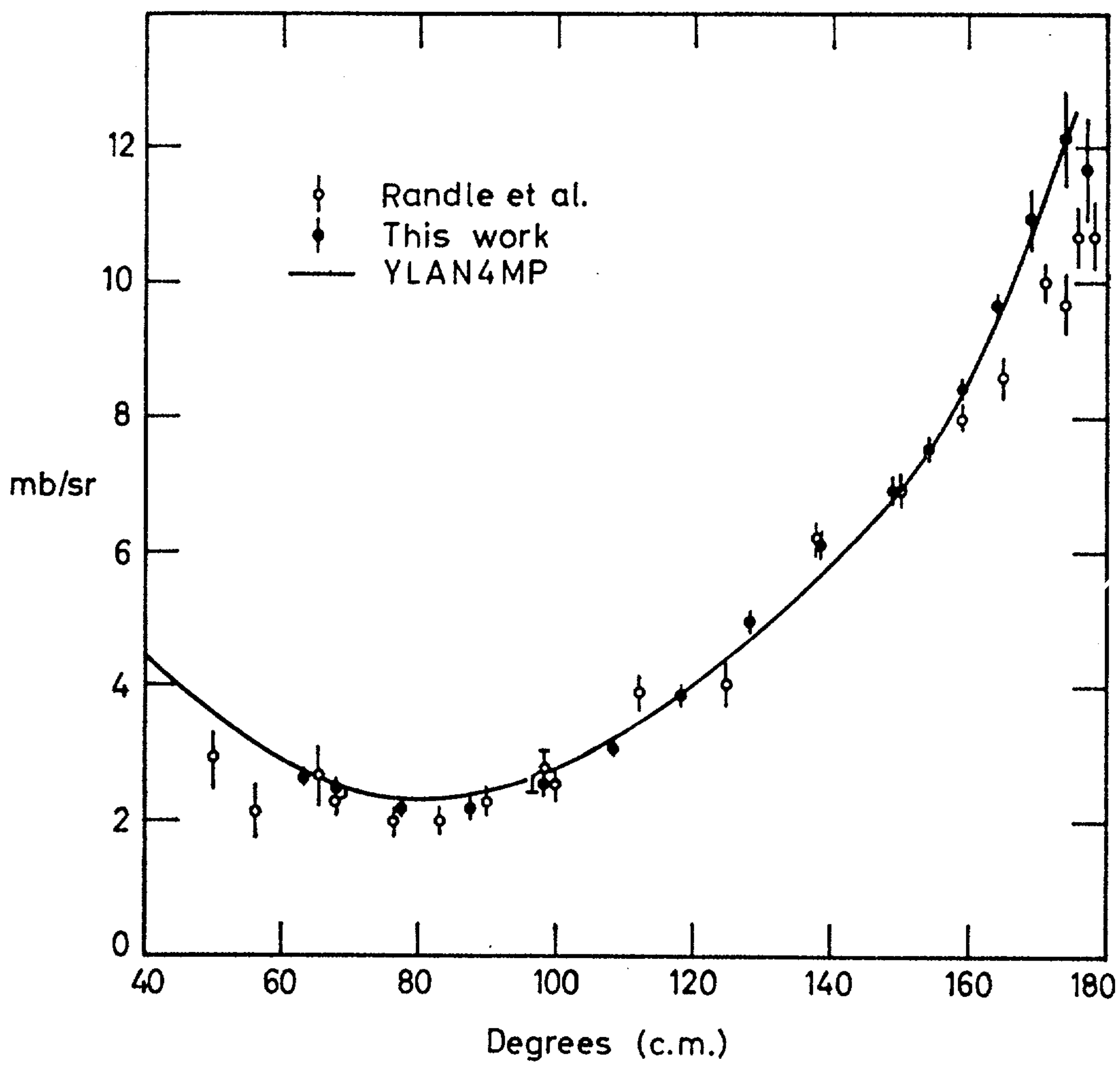

FIG. 6. The 150-MeV data normalized to YLAN4MP.

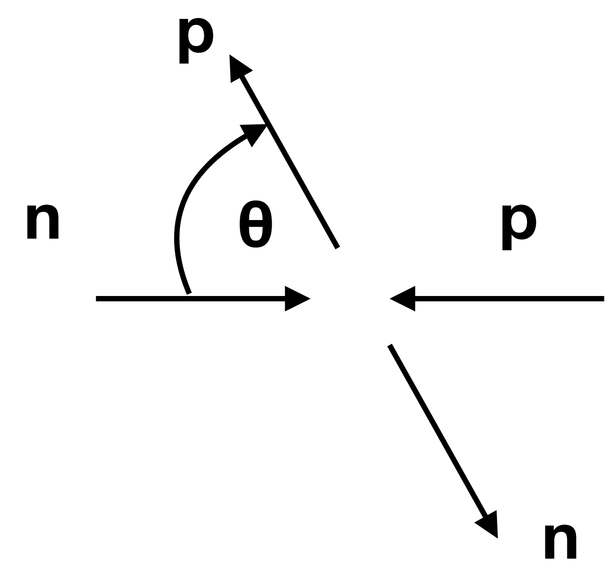

per confronto scattering di Rutherford, manca risalita a $\theta = \pi$

$$\frac{d\sigma}{d\Omega} = r_e^2 \ (zZ)^2 \ \frac{(m_e c^2)^2}{4p^2 v^2 \sin^4 \theta/2}$$

1. PHYSICAL CONSTANTS

Table 1.1. Reviewed 2015 by P.J. Mohr and D.B. Newell (NIST). Mainly from the "CODATA Recommended Values of the Fundamental Physical Constants: 2014" by P.J. Mohr, D.B. Newell, and B.N. Taylor in arXiv:1507.07956 (2015) and RMP (to be submitted). The last group of constants (beginning with the Fermi coupling constant) comes from the Particle Data Group. The figures in parentheses after the values give the 1-standard-deviation uncertainties in the last digits; the corresponding fractional uncertainties in parts per 10^9 (ppb) are given in the last column. This set of constants (aside from the last group) is recommended for international use by CODATA (the Committee on Data for Science and Technology). The full 2014 CODATA set of constants may be found at `http://physics.nist.gov/constants`. See also P.J. Mohr and D.B. Newell, "Resource Letter FC-1: The Physics of Fundamental Constants," Am. J. Phys. **78**, 338 (2010).

Quantity	Symbol, equation	Value	Uncertainty (ppb)
speed of light in vacuum	c	299 792 458 m s^{-1}	exact*
Planck constant	h	6.626 070 040(81)$\times 10^{-34}$ J s	12
Planck constant, reduced	$\hbar \equiv h/2\pi$	1.054 571 800(13)$\times 10^{-34}$ J s	12
		= 6.582 119 514(40)$\times 10^{-22}$ MeV s	6.1
electron charge magnitude	e	1.602 176 6208(98)$\times 10^{-19}$ C = 4.803 204 673(30)$\times 10^{-10}$ esu	6.1, 6.1
conversion constant	$\hbar c$	197.326 9788(12) MeV fm	6.1
conversion constant	$(\hbar c)^2$	0.389 379 3656(48) GeV^2 mbarn	12
electron mass	m_e	0.510 998 9461(31) MeV/c^2 = 9.109 383 56(11)$\times 10^{-31}$ kg	6.2, 12
proton mass	m_p	938.272 0813(58) MeV/c^2 = 1.672 621 898(21)$\times 10^{-27}$ kg	6.2, 12
		= 1.007 276 466 879(91) u = 1836.152 673 89(17) m_e	0.090, 0.095
deuteron mass	m_d	1875.612 928(12) MeV/c^2	6.2
unified atomic mass unit (u)	(mass ^{12}C atom)/12 = (1 g)/(N_A mol)	931.494 0954(57) MeV/c^2 = 1.660 539 040(20)$\times 10^{-27}$ kg	6.2, 12
permittivity of free space	$\epsilon_0 = 1/\mu_0 c^2$	8.854 187 817 ... $\times 10^{-12}$ F m^{-1}	exact
permeability of free space	μ_0	$4\pi \times 10^{-7}$ N A^{-2} = 12.566 370 614 ... $\times 10^{-7}$ N A^{-2}	exact
fine-structure constant	$\alpha = e^2/4\pi\epsilon_0\hbar c$	7.297 352 5664(17)$\times 10^{-3}$ = 1/137.035 999 139(31)†	0.23, 0.23
classical electron radius	$r_e = e^2/4\pi\epsilon_0 m_e c^2$	2.817 940 3227(19)$\times 10^{-15}$ m	0.68
(e^- Compton wavelength)/2π	$\lambda\!\!\!^{-}_e = \hbar/m_e c = r_e \alpha^{-1}$	3.861 592 6764(18)$\times 10^{-13}$ m	0.45
Bohr radius ($m_{\text{nucleus}} = \infty$)	$a_\infty = 4\pi\epsilon_0\hbar^2/m_e e^2 = r_e \alpha^{-2}$	0.529 177 210 67(12)$\times 10^{-10}$ m	0.23
wavelength of 1 eV/c particle	$hc/(1\text{ eV})$	1.239 841 9739(76)$\times 10^{-6}$ m	6.1
Rydberg energy	$hcR_\infty = m_e e^4/2(4\pi\epsilon_0)^2\hbar^2 = m_e c^2\alpha^2/2$	13.605 693 009(84) eV	6.1
Thomson cross section	$\sigma_T = 8\pi r_e^2/3$	0.665 245 871 58(91) barn	1.4
Bohr magneton	$\mu_B = e\hbar/2m_e$	5.788 381 8012(26)$\times 10^{-11}$ MeV T^{-1}	0.45
nuclear magneton	$\mu_N = e\hbar/2m_p$	3.152 451 2550(15)$\times 10^{-14}$ MeV T^{-1}	0.46
electron cyclotron freq./field	$\omega^e_{\text{cycl}}/B = e/m_e$	1.758 820 024(11)$\times 10^{11}$ rad s^{-1} T^{-1}	6.2
proton cyclotron freq./field	$\omega^p_{\text{cycl}}/B = e/m_p$	9.578 833 226(59)$\times 10^{7}$ rad s^{-1} T^{-1}	6.2
gravitational constant‡	G_N	6.674 08(31)$\times 10^{-11}$ m^3 kg^{-1} s^{-2}	4.7×10^4
		= 6.708 61(31)$\times 10^{-39}$ $\hbar c$ (GeV/c^2)$^{-2}$	4.7×10^4
standard gravitational accel.	g_N	9.806 65 m s^{-2}	exact
Avogadro constant	N_A	6.022 140 857(74)$\times 10^{23}$ mol^{-1}	12
Boltzmann constant	k	1.380 648 52(79)$\times 10^{-23}$ J K^{-1}	570
		= 8.617 3303(50)$\times 10^{-5}$ eV K^{-1}	570
molar volume, ideal gas at STP	$N_A k$(273.15 K)/(101 325 Pa)	22.413 962(13)$\times 10^{-3}$ m^3 mol^{-1}	570
Wien displacement law constant	$b = \lambda_{\max} T$	2.897 7729(17)$\times 10^{-3}$ m K	570
Stefan-Boltzmann constant	$\sigma = \pi^2 k^4/60\hbar^3 c^2$	5.670 367(13)$\times 10^{-8}$ W m^{-2} K^{-4}	2300
Fermi coupling constant**	$G_F/(\hbar c)^3$	1.166 378 7(6)$\times 10^{-5}$ GeV^{-2}	500
weak-mixing angle	$\sin^2\hat{\theta}(M_Z)$ ($\overline{\text{MS}}$)	0.231 29(5)††	2.2×10^5
$W^\pm$ boson mass	m_W	80.385(15) GeV/c^2	1.9×10^5
Z^0 boson mass	m_Z	91.1876(21) GeV/c^2	2.3×10^4
strong coupling constant	$\alpha_s(m_Z)$	0.1181(11)	1.0×10^7

π = 3.141 592 653 589 793 238   e = 2.718 281 828 459 045 235 γ = 0.577 215 664 901 532 861

1 in ≡ 0.0254 m	1 G ≡ 10^{-4} T	1 eV = 1.602 176 6208(98) $\times 10^{-19}$ J	kT at 300 K = [38.681 740(22)]$^{-1}$ eV
1 Å ≡ 0.1 nm	1 dyne ≡ 10^{-5} N	1 eV/c^2 = 1.782 661 907(11) $\times 10^{-36}$ kg	0 °C ≡ 273.15 K
1 barn ≡ 10^{-28} m^2	1 erg ≡ 10^{-7} J	2.997 924 58 $\times 10^9$ esu = 1 C	1 atmosphere ≡ 760 Torr ≡ 101 325 Pa

* The meter is the length of the path traveled by light in vacuum during a time interval of 1/299 792 458 of a second.
† At $Q^2 = 0$. At $Q^2 \approx m_W^2$ the value is ~ 1/128.
‡ Absolute lab measurements of G_N have been made only on scales of about 1 cm to 1 m.
** See the discussion in Sec. 10, "Electroweak model and constraints on new physics."
†† The corresponding $\sin^2\theta$ for the effective angle is 0.23155(5).

Figure 4.42: da S.Eidelman *et al.*, Physics Letters B592, 1, 2004

Table 4.1. Revised June 2016 by D.E. Groom (LBNL). The atomic number (top left) is the number of protons in the nucleus. The atomic masses (bottom) of stable elements are weighted by isotopic abundances in the Earth's surface. Atomic masses are relative to the mass of ^{12}C, defined to be exactly 12 unified atomic mass units (u) (approx. g/mole). The exceptions are Th, Pa, and U, which have no stable isotopes but do have characteristic terrestrial compositions. Relative isotopic abundances often vary considerably, both in natural and commercial samples; this is reflected in the number of significant figures given for the mass. Masses may be found at `http://physics.nist.gov/cgi-bin/Compositions/stand_alone.pl` . If there is no stable isotope the atomic mass of the most stable isotope is given in parentheses.

IUPAC announced verification of the discoveries of elements 113, 115, 117, and 118 in December 2015. Provisional names were assigned in June 2016. The 7th period of the periodic table is now complete.

PERIODIC TABLE OF THE ELEMENTS

1 IA	2 IIA	3 IIIB	4 IVB	5 VB	6 VIB	7 VIIB	8	9 VIII	10	11 IB	12 IIB	13 IIIA	14 IVA	15 VA	16 VIA	17 VIIA	18 VIIIA
1 H hydrogen 1.008																	2 He helium 4.002602
3 Li lithium 6.94	4 Be beryllium 9.012182											5 B boron 10.81	6 C carbon 12.0107	7 N nitrogen 14.007	8 O oxygen 15.999	9 F fluorine 18.998403163	10 Ne neon 20.1797
11 Na sodium 22.98976928	12 Mg magnesium 24.305											13 Al aluminum 26.9815385	14 Si silicon 28.085	15 P phosphorus 30.973761998	16 S sulfur 32.06	17 Cl chlorine 35.45	18 Ar argon 39.948
19 K potassium 39.0983	20 Ca calcium 40.078	21 Sc scandium 44.955908	22 Ti titanium 47.867	23 V vanadium 50.9415	24 Cr chromium 51.9961	25 Mn manganese 54.938044	26 Fe iron 55.845	27 Co cobalt 58.933195	28 Ni nickel 58.6934	29 Cu copper 63.546	30 Zn zinc 65.38	31 Ga gallium 69.723	32 Ge germanium 72.630	33 As arsenic 74.921595	34 Se selenium 78.971	35 Br bromine 79.904	36 Kr krypton 83.798
37 Rb rubidium 85.4678	38 Sr strontium 87.62	39 Y yttrium 88.90584	40 Zr zirconium 91.224	41 Nb niobium 92.90637	42 Mo molybdenum 95.95	43 Tc technetium (97.907212)	44 Ru ruthenium 101.07	45 Rh rhodium 102.90550	46 Pd palladium 106.42	47 Ag silver 107.8682	48 Cd cadmium 112.414	49 In indium 114.818	50 Sn tin 118.710	51 Sb antimony 121.760	52 Te tellurium 127.60	53 I iodine 126.90447	54 Xe xenon 131.293
55 Cs caesium 132.90545196	56 Ba barium 137.327	57–71 LANTHA- NIDES	72 Hf hafnium 178.49	73 Ta tantalum 180.94788	74 W tungsten 183.84	75 Re rhenium 186.207	76 Os osmium 190.23	77 Ir iridium 192.217	78 Pt platinum 195.084	79 Au gold 196.966569	80 Hg mercury 200.592	81 Tl thallium 204.38	82 Pb lead 207.2	83 Bi bismuth 208.98040	84 Po polonium (208.98243)	85 At astatine (209.98715)	86 Rn radon (222.01758)
87 Fr francium (223.01974)	88 Ra radium (226.02541)	89–103 ACTINIDES	104 Rf rutherford. (267.12169)	105 Db dubnium (268.12567)	106 Sg seaborgium (271.13393)	107 Bh bohrium (272.13826)	108 Hs hassium (270.13429)	109 Mt meitnerium (276.15159)	110 Ds darmstadt. (281.16451)	111 Rg roentgen. (280.16514)	112 Cn copernicium (285.17712)	113 Nh (nihonium) (284.17873)	114 Fl flerovium (289.19042)	115 Mc (moscovium) (288.19274)	116 Lv livermorium (293.20449)	117 Ts (tennessine) (292.20746)	118 Og (oganesson) (294.21392)

Lanthanide series	57 La lanthanum 138.90547	58 Ce cerium 140.116	59 Pr praseodym. 140.90766	60 Nd neodymium 144.242	61 Pm promethium (144.91276)	62 Sm samarium 150.36	63 Eu europium 151.964	64 Gd gadolinum 157.25	65 Tb terbium 158.92535	66 Dy dysprosium 162.500	67 Ho holmium 164.93033	68 Er erbium 167.259	69 Tm thulium 168.93422	70 Yb ytterbium 173.054	71 Lu lutetium 174.9668
Actinide series	89 Ac actinium (227.02775)	90 Th thorium 232.0377	91 Pa protactinium 231.03588	92 U uranium 238.02891	93 Np neptunium (237.04817)	94 Pu plutonium (244.06420)	95 Am americium (243.06138)	96 Cm curium (247.07035)	97 Bk berkelium (247.07031)	98 Cf californium (251.07959)	99 Es einsteinium (252.08298)	100 Fm fermium (257.09511)	101 Md mendelevium (258.09844)	102 No nobelium (259.10103)	103 Lr lawrencium (262.10961)

Figure 4.43: da S.Eidelman *et al.*, Physics Letters B592, 1, 2004

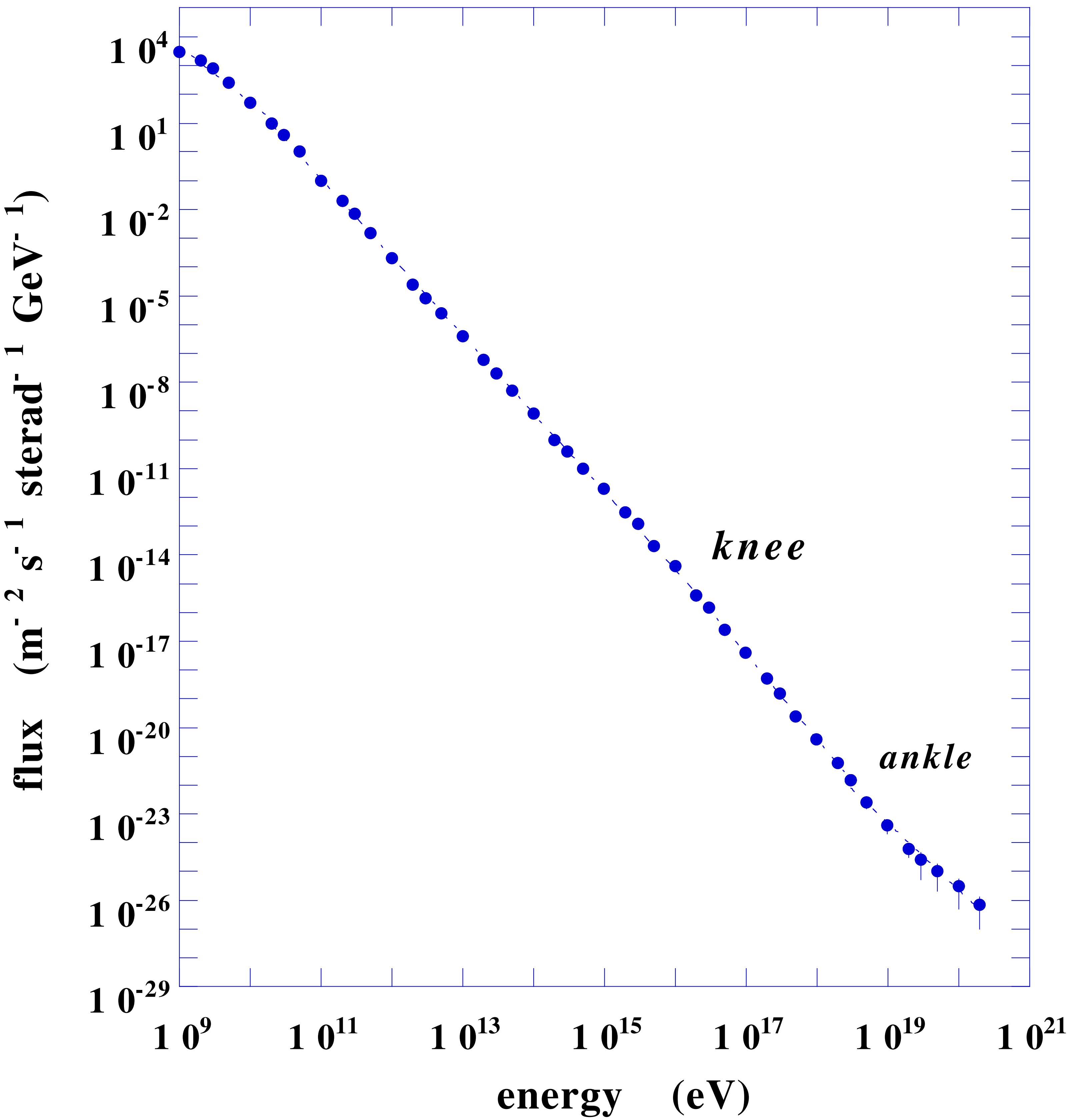

Figure 3.2: Flusso dei raggi cosmici primari

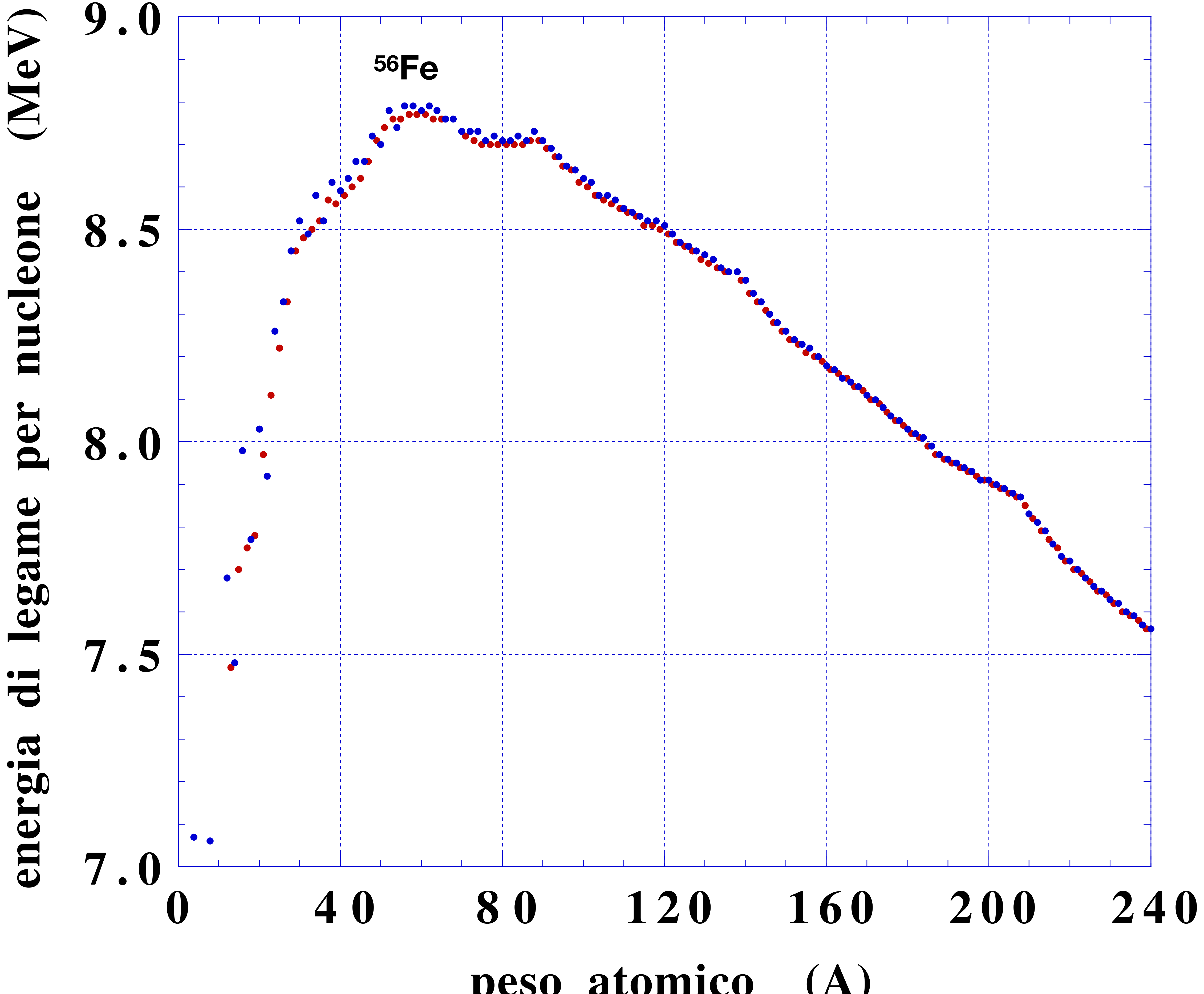

energia di legame per nucleone (MeV)
9.0
8.5
8.0
7.5
7.0
56Fe
0
40
80
120
160
200
240
peso atomico (A)

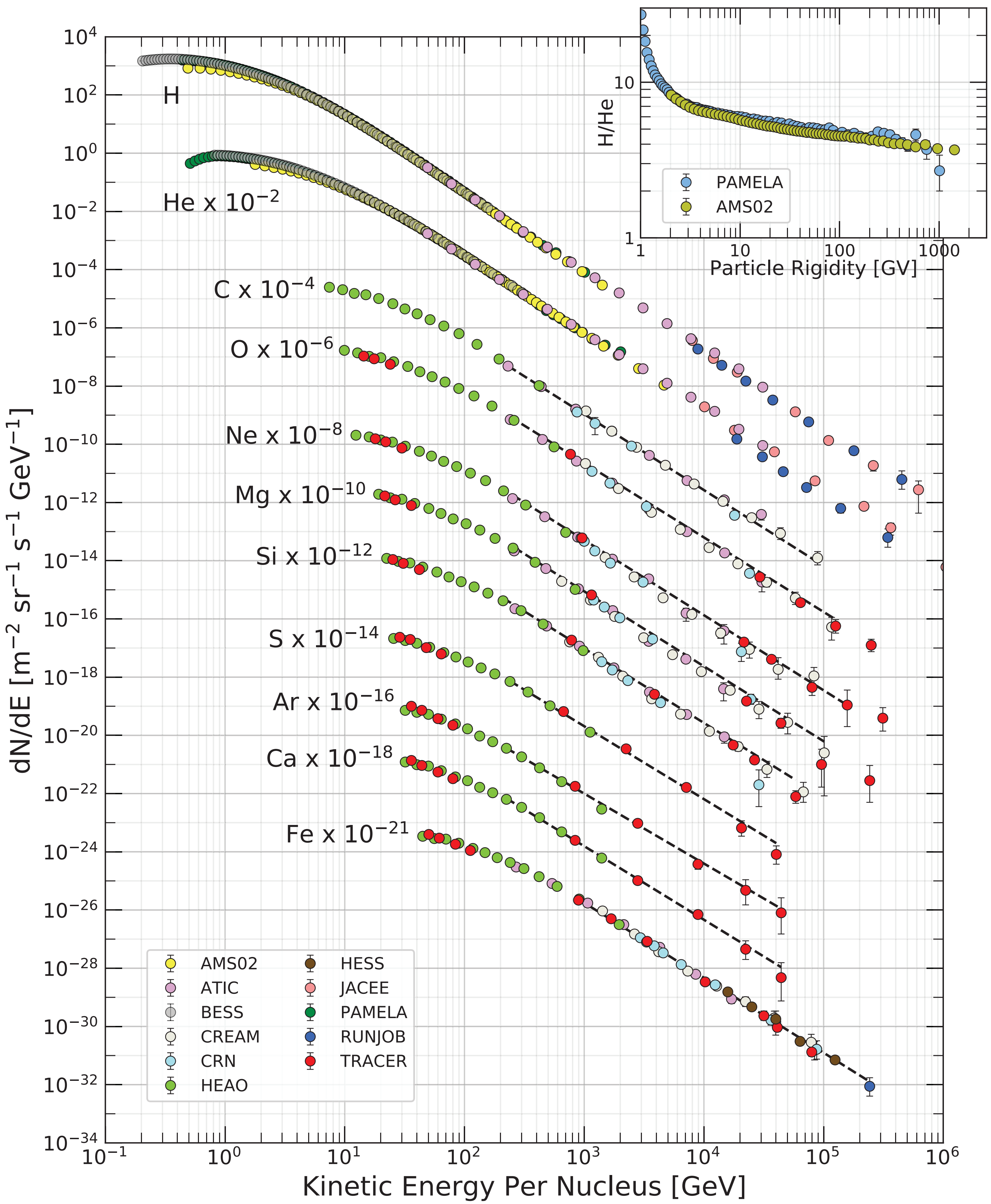

Figure 29.1: Fluxes of nuclei of the primary cosmic radiation in particles per energy-per-nucleus are plotted vs energy-per-nucleus using data from Refs. [2–13]. The inset shows the H/He ratio at constant rigidity [2,4].

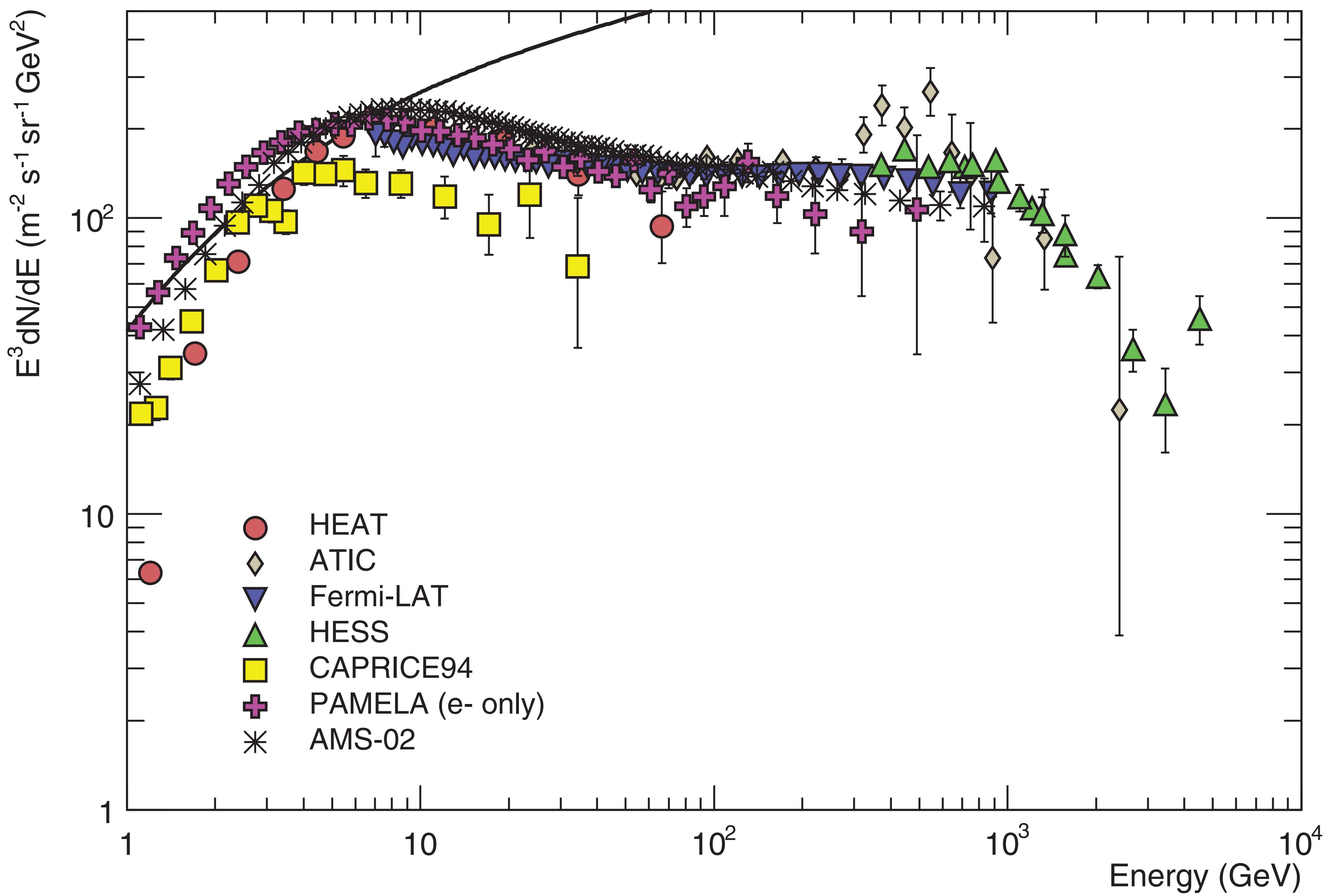

Figure 29.2: Differential spectrum of electrons plus positrons (except PAMELA data, which are electrons only) multiplied by E^3 [19–23,33,34]. The line shows the proton spectrum [25] multiplied by 0.01.

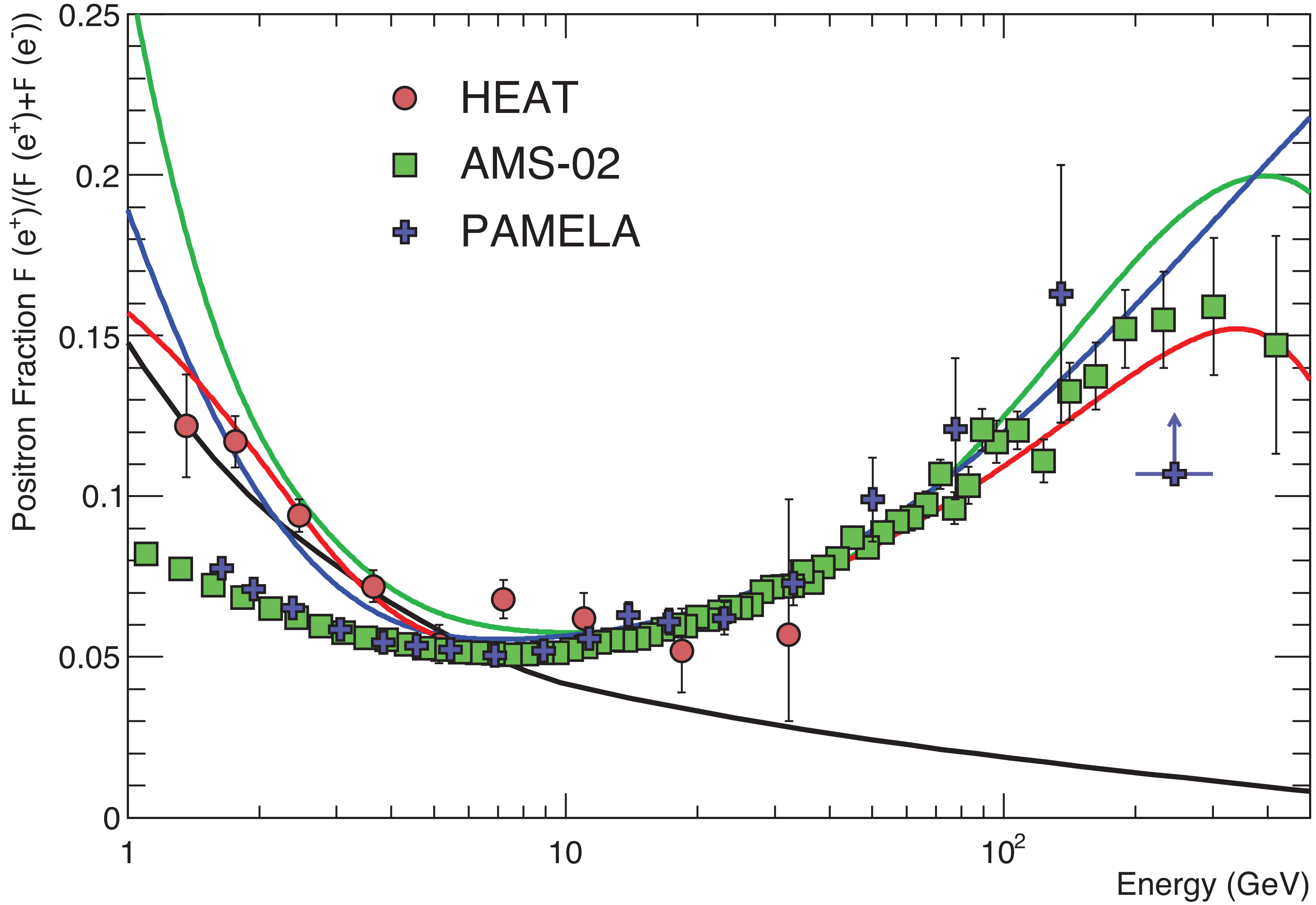

Figure 29.3: The positron fraction (ratio of the flux of e^+ to the total flux of e^+ and e^-) [26,24,30]. The heavy black line is a model of pure secondary production [28] and the three thin lines show three representative attempts to model the positron excess with different phenomena: green: dark matter decay [29]; blue: propagation physics [32]; red: production in pulsars [40]. The ratio below 10 GeV is dependent on the polarity of the solar magnetic field.

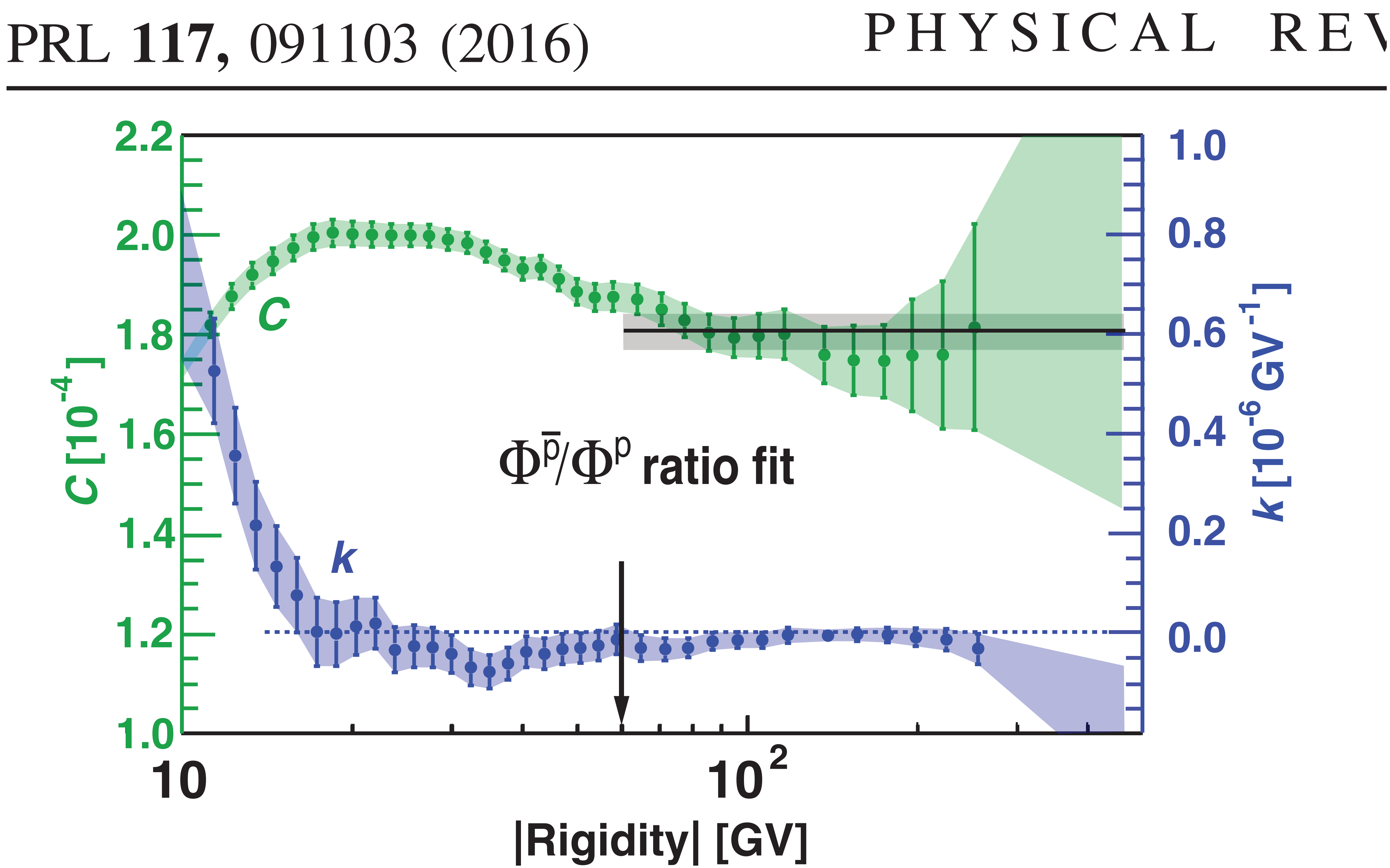

Rigidity = pc/Ze   [Rigidity] = [Energia]/[Carica] = [Volt]

AMS ha riportato anche un candidato di anti-Elio 3 e anti-Elio 4 (dubbi sull'origine)

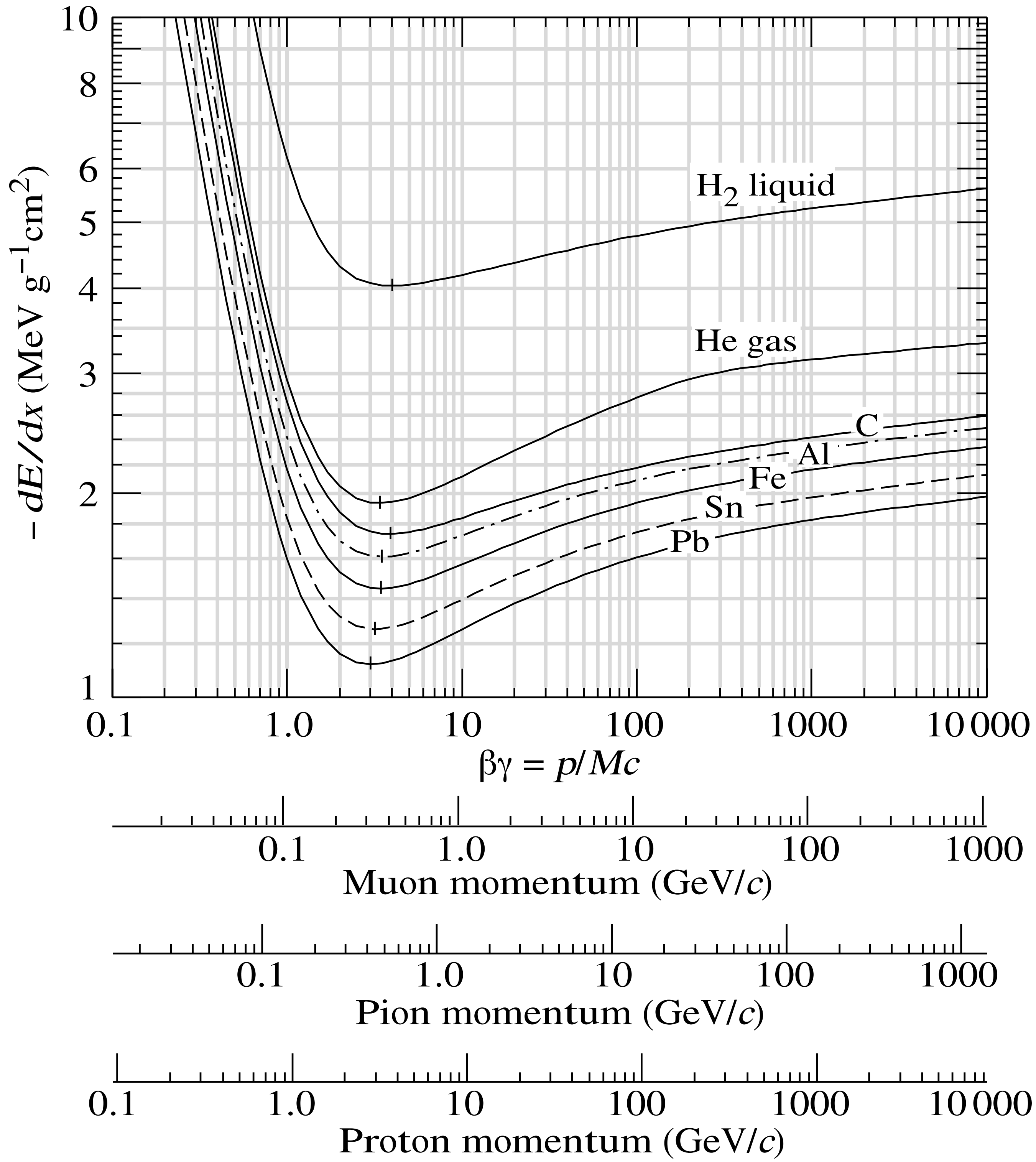

Figure 1.43: $(dE/dx)_{ion}$ in diversi materiali in funzione di $\beta\gamma$ per particelle di carica $z = 1$ (S.Eidelman *et al.*, Physics Letters B592, 1, 2004)

NOVEMBER 1 AND 15, 1942 PHYSICAL REVIEW VOLUM

Experimental Determination of the Disintegration Curve of Mesotrons

BRUNO ROSSI AND NORRIS NERESON
Cornell University, Ithaca, New York

(Received September 17, 1942)

The disintegration curve of mesotrons has been experimentally determined by investigating the delayed emission of disintegration electrons which takes place after the absorption of mesotrons by matter. Within the experimental errors, the disintegration curve is exponential and corresponds to a mean lifetime of 2.3±0.2 microseconds.

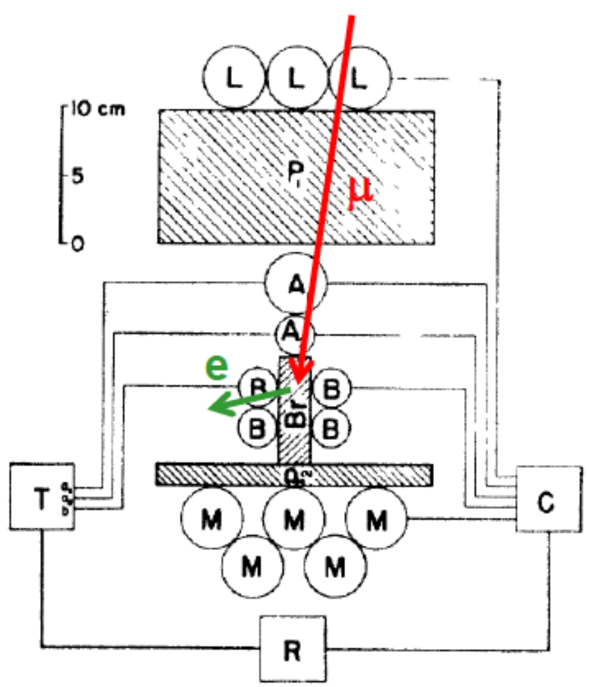

L, A, B, M: Geiger-Muller counters
the 4 counters L are connected in parallel (OR)
the same for the 4 counters B and the 5 counters M

Br: brass plate 25.5x8x2.3 cm
compromise: rate of stopped muons vs probability of detecting the electron

good event:
muon gives signal in L, A1, A2
decays in Br → no signal in M, B
decay electron gives a signal in B

C gives a signal which activates R if
$L \cdot A1 \cdot A2 \cdot B \cdot \overline{M}$ (10^{-4} s)
R registers the amplitude of the signal from T proportional to Δt between A and B

P1: 9 cm of lead
to cut the electron component
P2: lead plate 1.4 cm thick
to decrease the probability of having a decay electron signal in M

Nereson Rossi

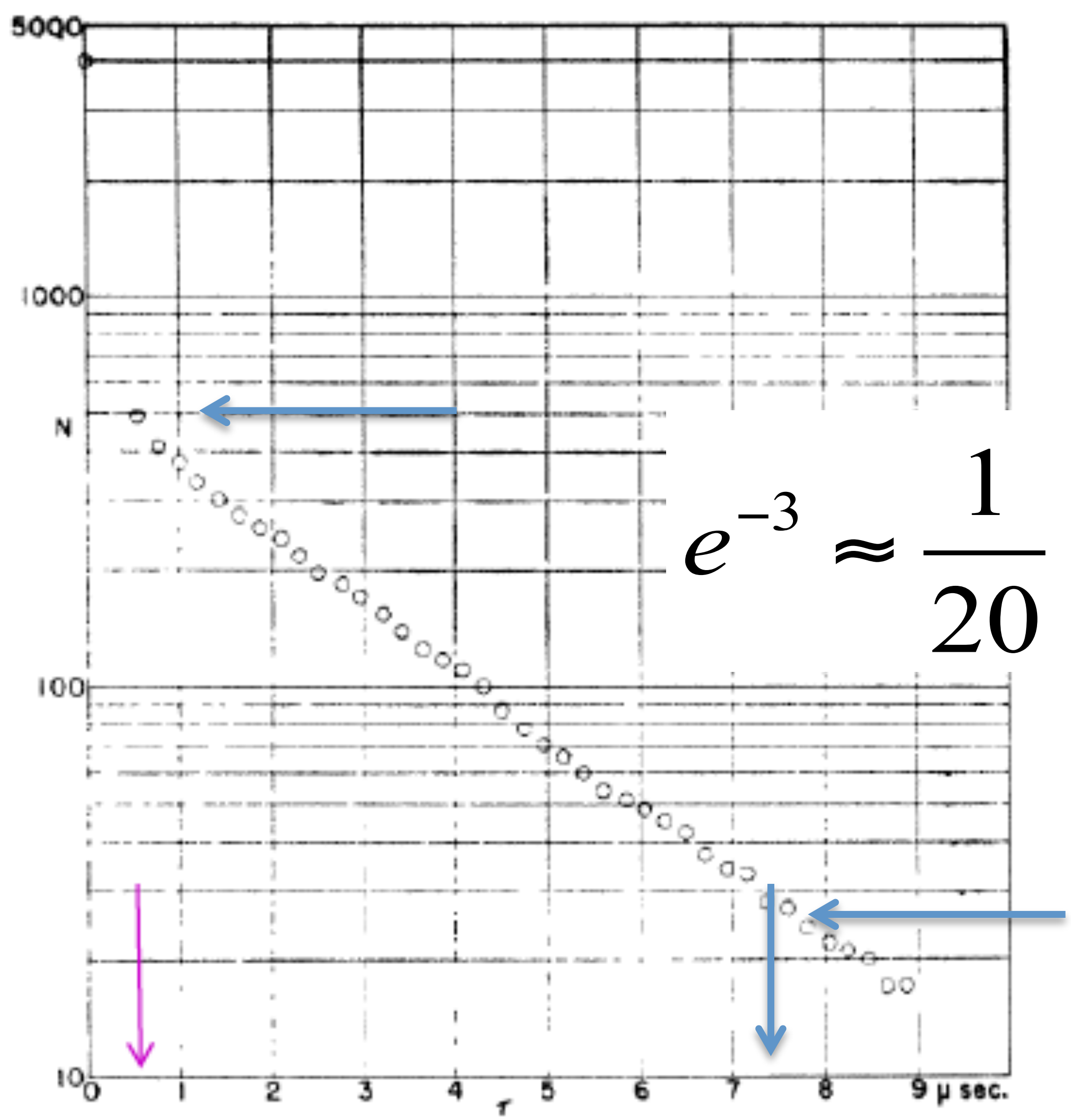

$$e^{-3} \approx \frac{1}{20}$$

FIG. 5. Experimental disintegration curve of mesotrons. The abscissa τ is the delay recorded by the time circuit, the ordinate is the logarithm of the number N of anti-coincidences accompanied by delays larger than the corresponding abscissa (Exp. A).

$\tau_{\mu}(\text{MuLan}) = 2196980.3(2.2)$ ps

PHYSICAL REVIEW D 87, 052003 (2013)

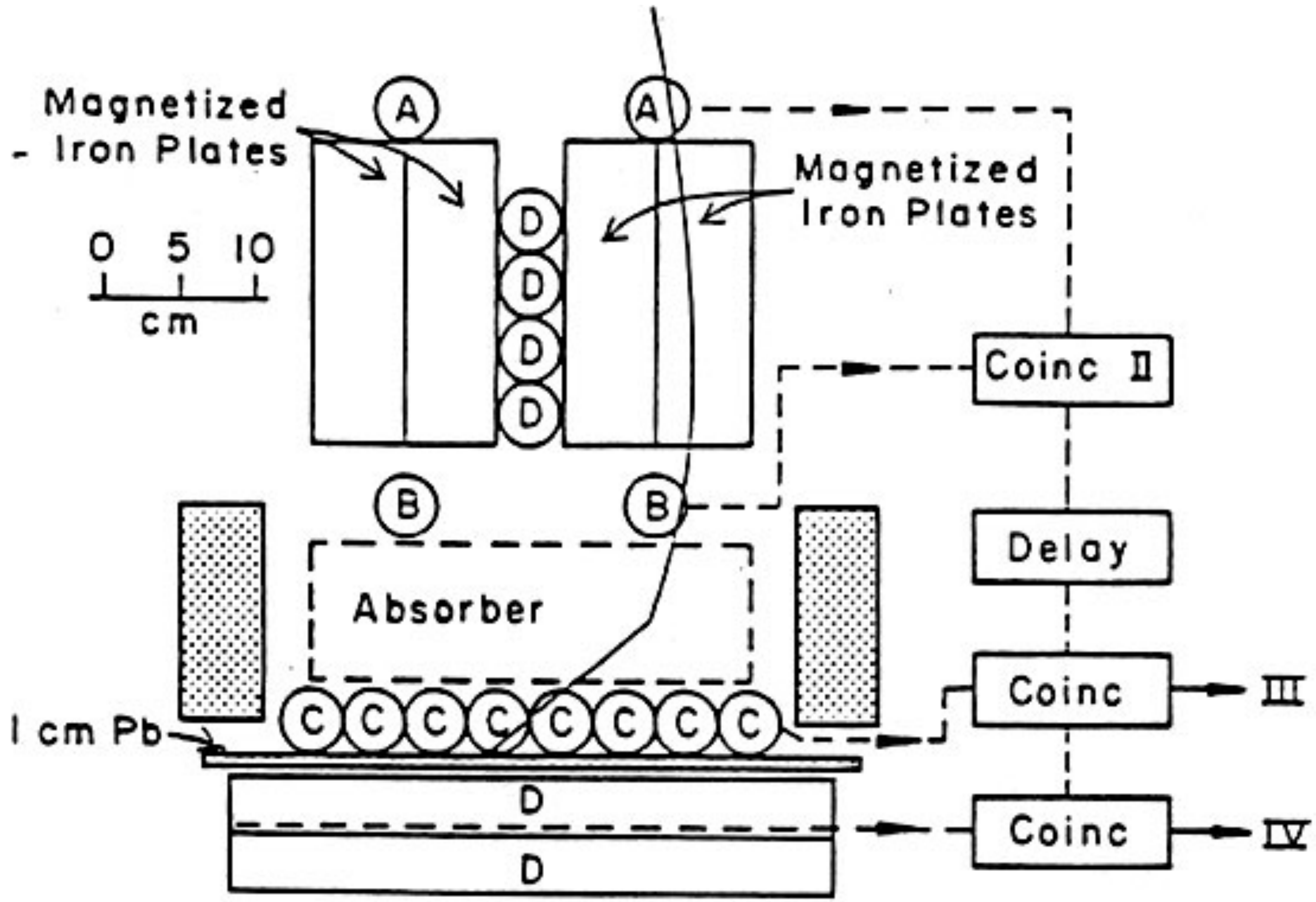

Figura 6.2: Schema originale dell'esperimento di Conversi, Pancini e Piccioni: l'arrivo del mesone è segnalato dalla coincidenza dei contatori A e B. Il campo magnetico permette di focalizzare una carica e defocalizzare la carica opposta. Il decadimento del mesone in un elettrone nell'assorbitore produce una coincidenza ritardata con i contatori C.

Perkins 1946: emulsioni su aereo, evento di interazione nucleare: $X + N \rightarrow p + {}^{3}H$

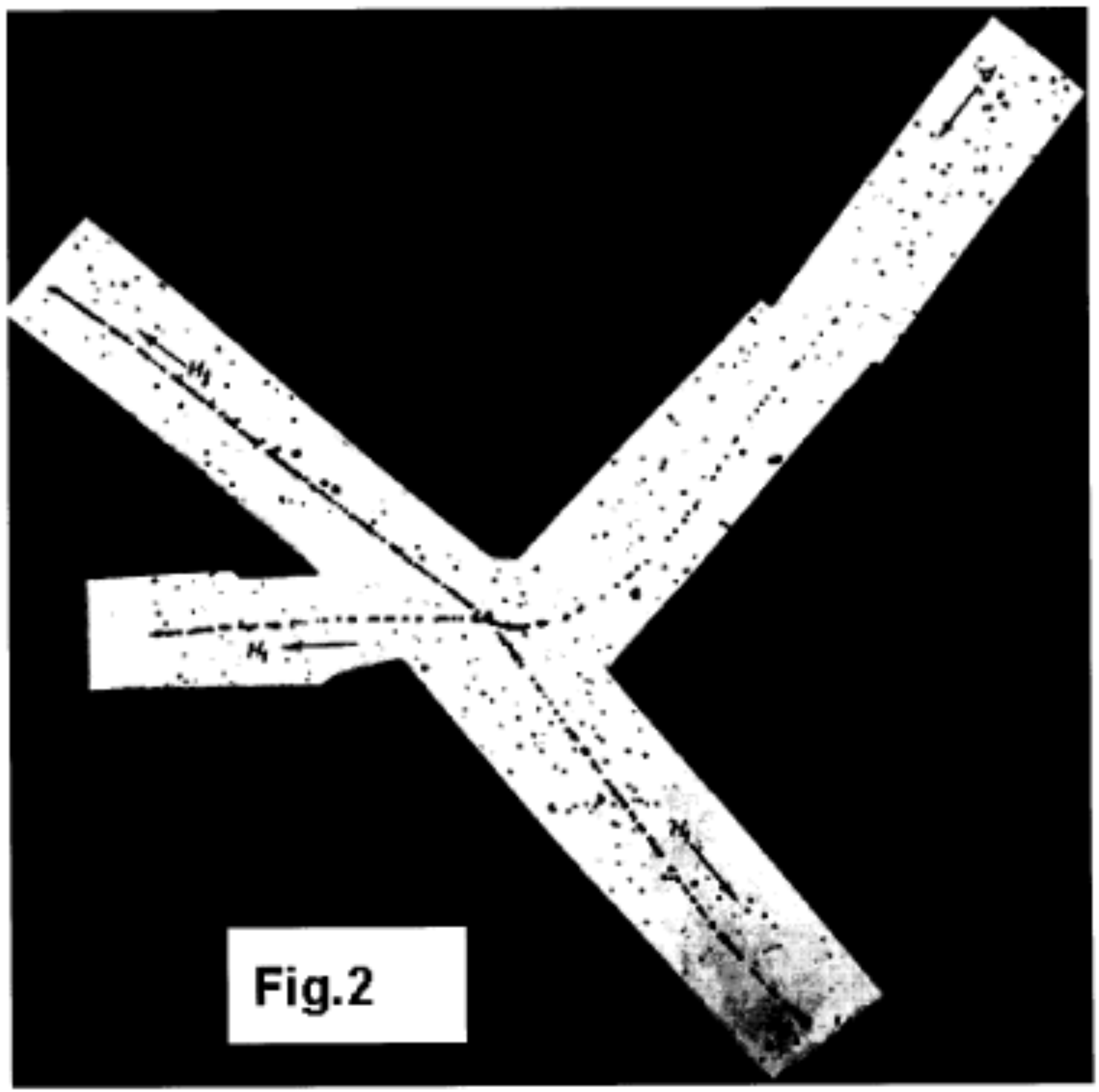

Fig.2

Slide di A. Zoccoli

Osservazione del π

(Lattes, Occhialini, Powell 1947)

- Per acquisire maggiori informazioni sui raggi cosmici voli con palloni in alta atmosfera.

- Utilizzo di emulsioni nucleari per registrare le interazioni.

- Powell ricevette il Nobel 1950
  - per la tecnica sperimentale
  - e per gli studi sui pioni fatti con questa tecnica

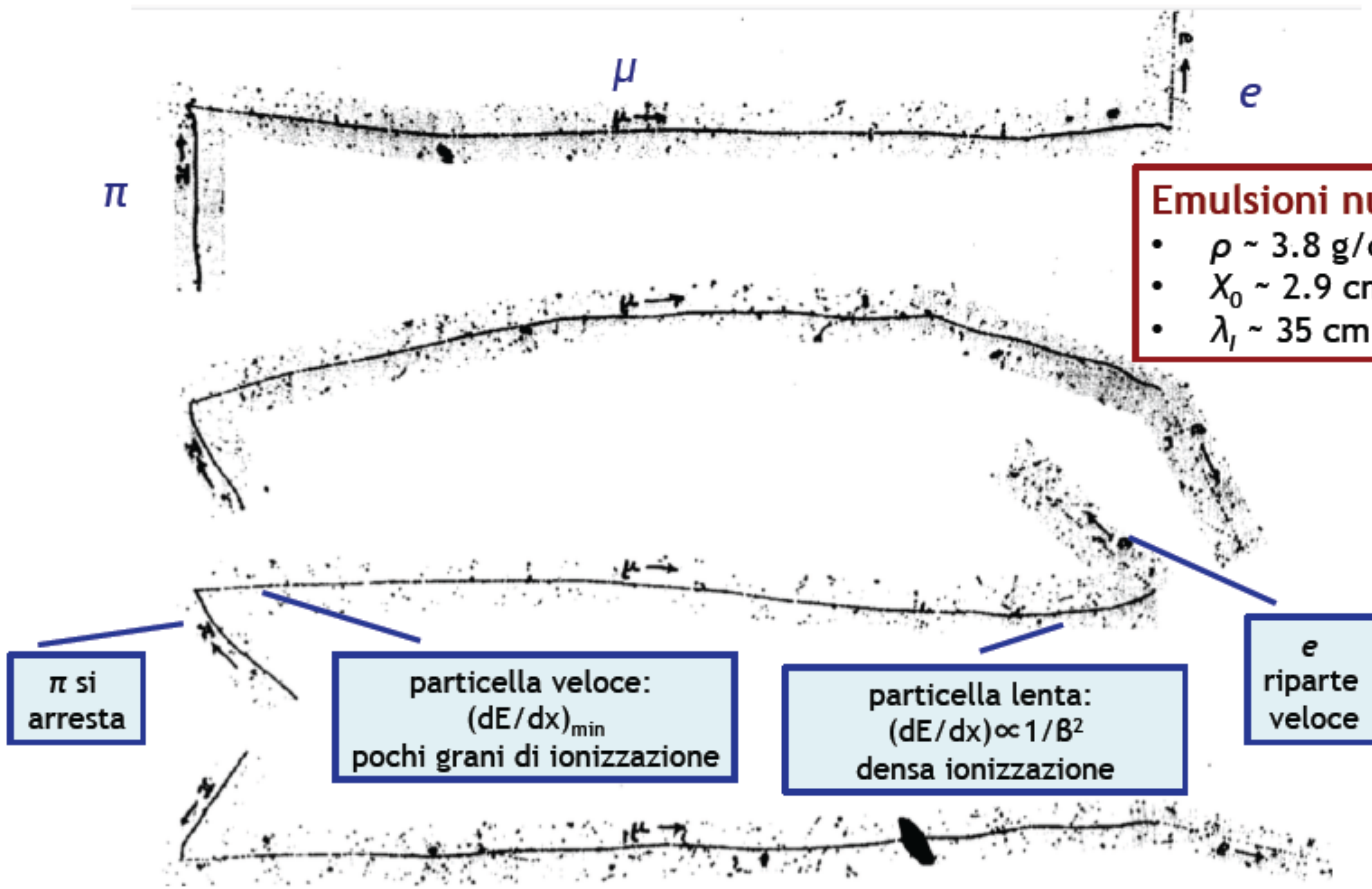

Emulsioni nucleari

- ρ ~ 3.8 g/cm^2
- X_0 ~ 2.9 cm
- λ_I ~ 35 cm

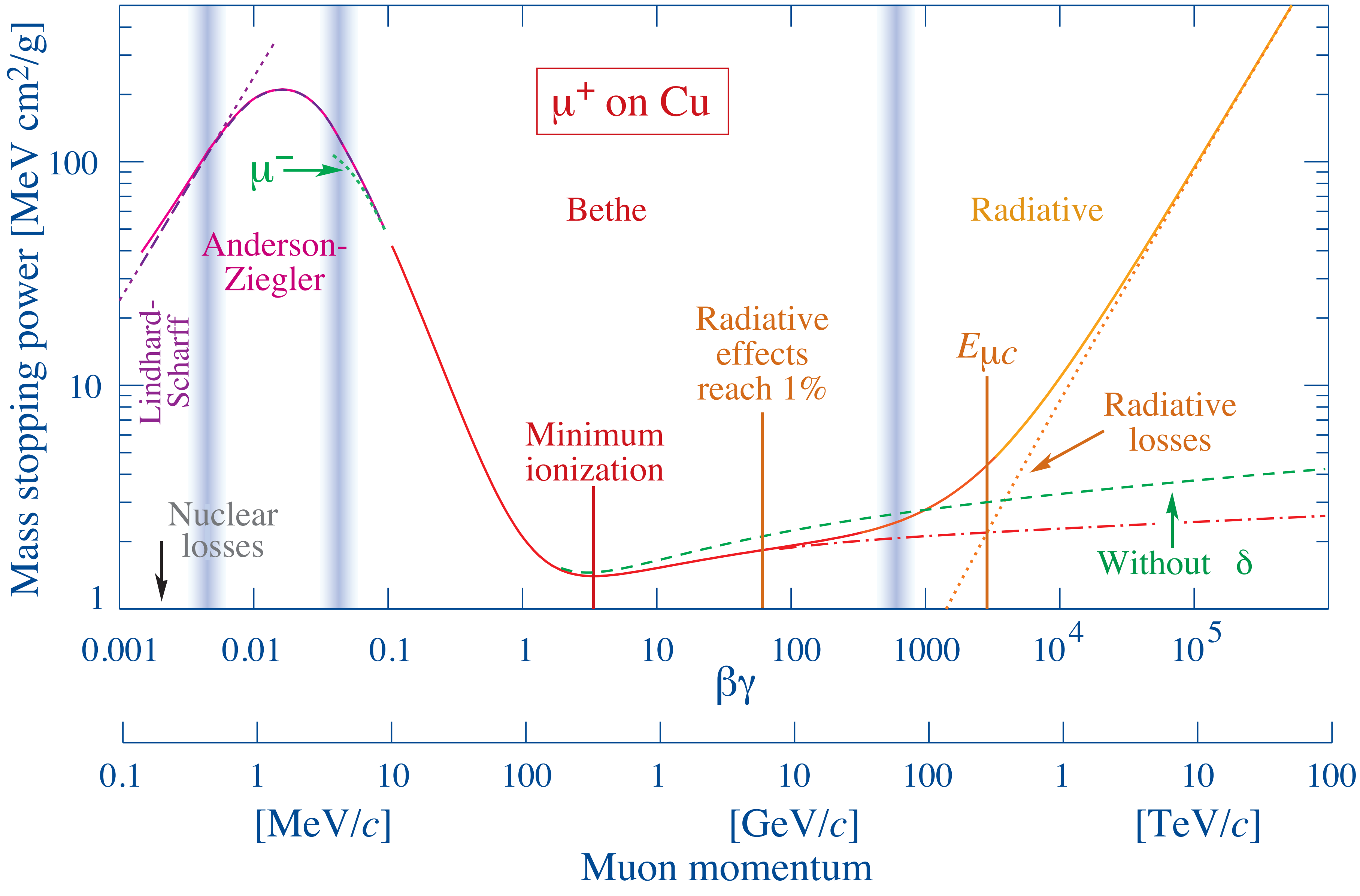

μ+ on Cu
μ−
Bethe
Radiative
Anderson-
Ziegler
Lindhard-
Scharff
Radiative
effects
reach 1%
Eμc
Radiative
losses
Minimum
ionization
Nuclear
losses
Without δ
Mass stopping power [MeV cm2/g]
1
10
100
0.001
0.01
0.1
1
10
100
1000
10^4
10^5
βγ
0.1
1
10
100
1
10
100
1
10
100
[MeV/c]
[GeV/c]
[TeV/c]
Muon momentum

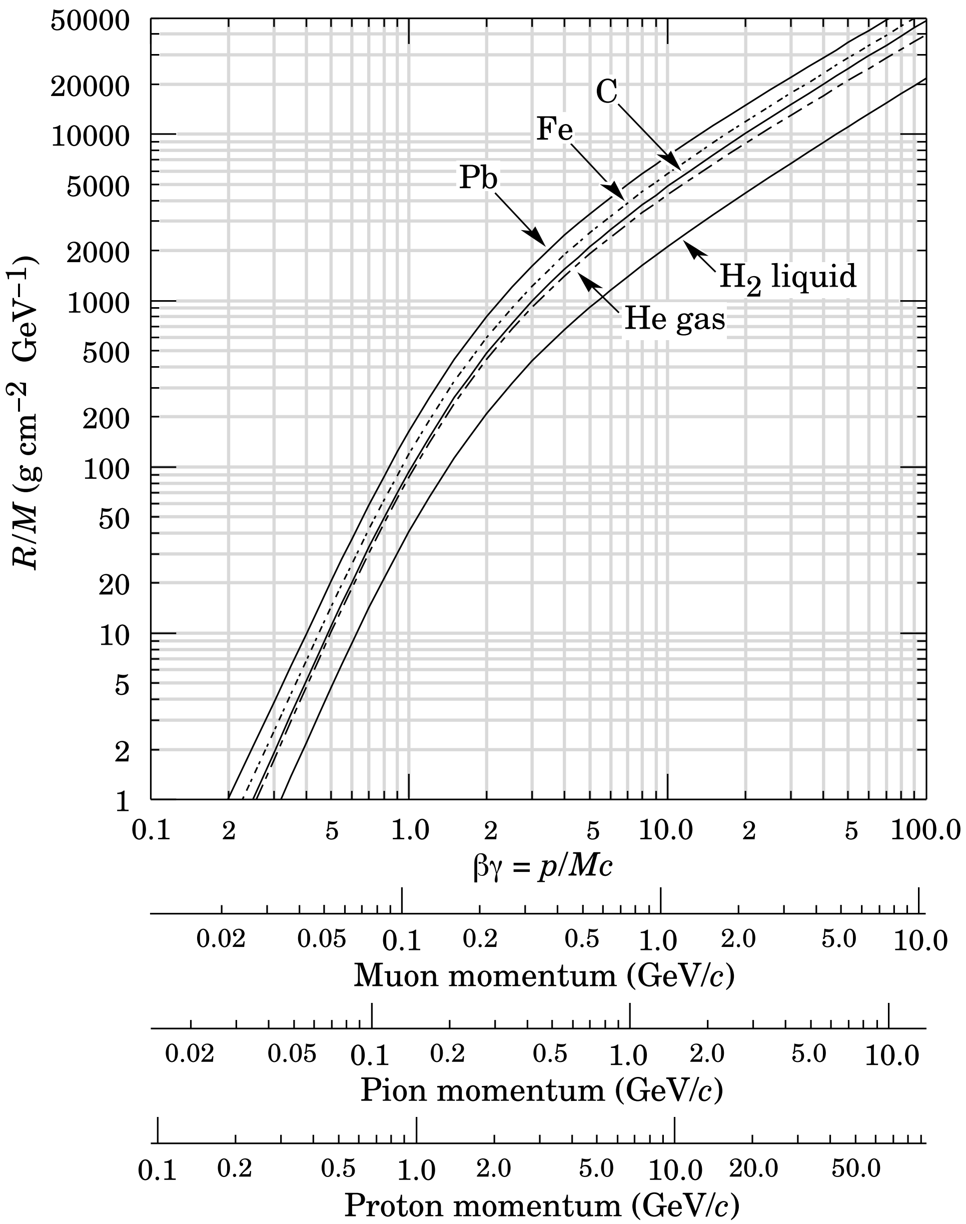

$$\frac{dE}{dx} = C \ \frac{Z}{A}\frac{z^2}{\beta^2}\left(\ln\frac{2mc^2\beta^2\gamma^2}{\langle I\rangle} - \beta^2\right)$$

$$R = \int_0^R dx = \int_{E_0}^0 \frac{dE}{dE/dx} \qquad\qquad dx = \rho d\ell$$

$$R = \int_{\beta_0}^0 \frac{Mc^2\gamma^3\beta d\beta}{z^2 f(\beta, Z, A)} = \frac{Mc^2}{z^2}\ F(\beta_0, Z, A)$$

Rochster 1947: Osserva la presenza di V in camera a nebbia
Particella neutra che decade in due particelle cariche

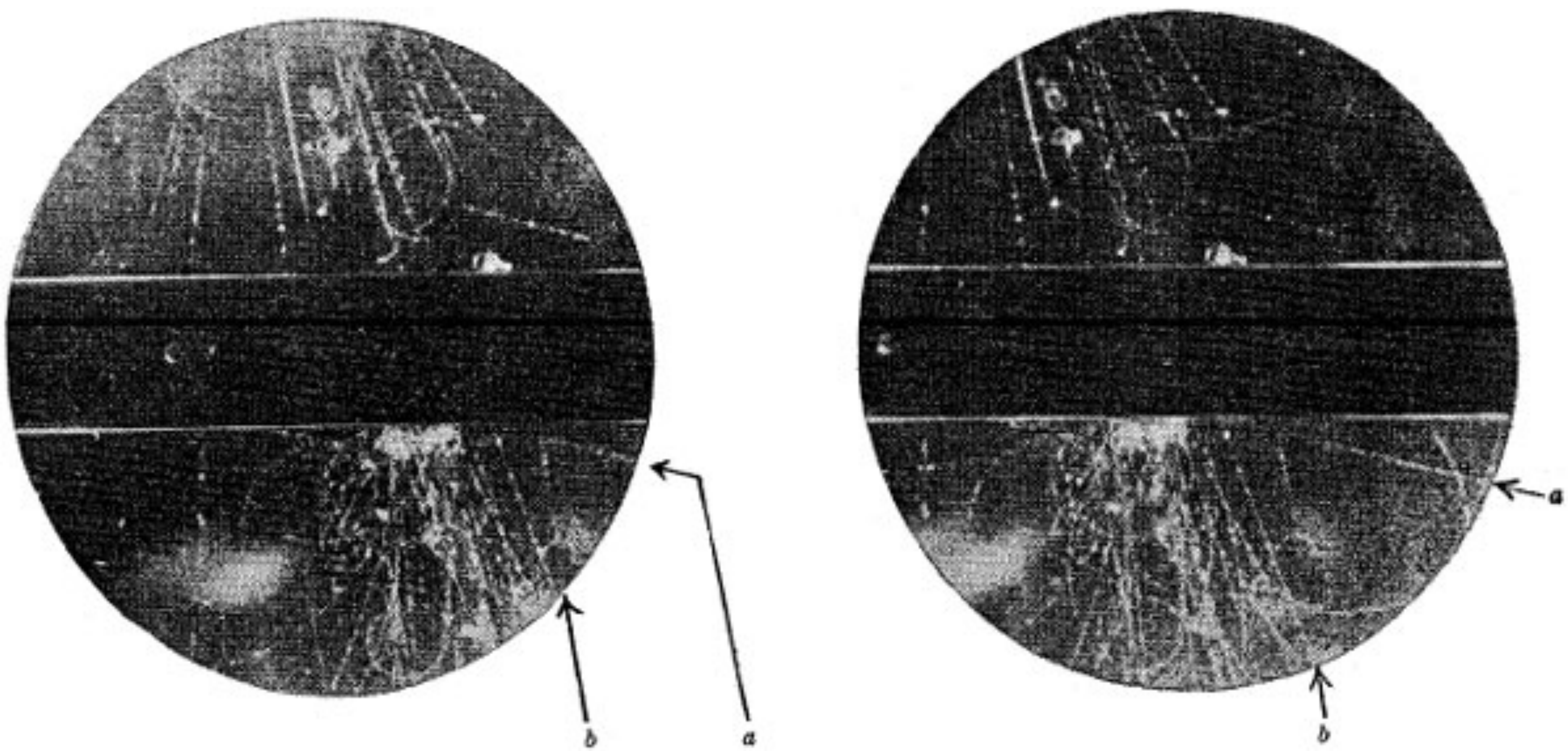

Camera a bolle
inventata da Donald Glaser 1952
Liquido a pressione minore della pressione di ebollizione (liquido surriscaldato)

Una particella carica interagendo con il liquido lo riscalda e lo trasforma in vapore creando bolle.

Le bolle sono fotografate.

Il pistone serve a comprimere e decomprimere il liquido per portarlo in condizioni di sovrariscaldamento.

Utlizzata tipicamente con idrogeno liquido per avere bersagli densi di protoni.

La pressione viene variata in corrispondenza di un segnale dall'acceleratore

Esempio di camera a bolle presso il CERN (BEBC)

Un’immagine di BEBC
Sciame elettromagnetico

Elettroni e positroni perdono energia rapidamente per irraggiamento creando in camera a bolle una tipica segnatura a spirale

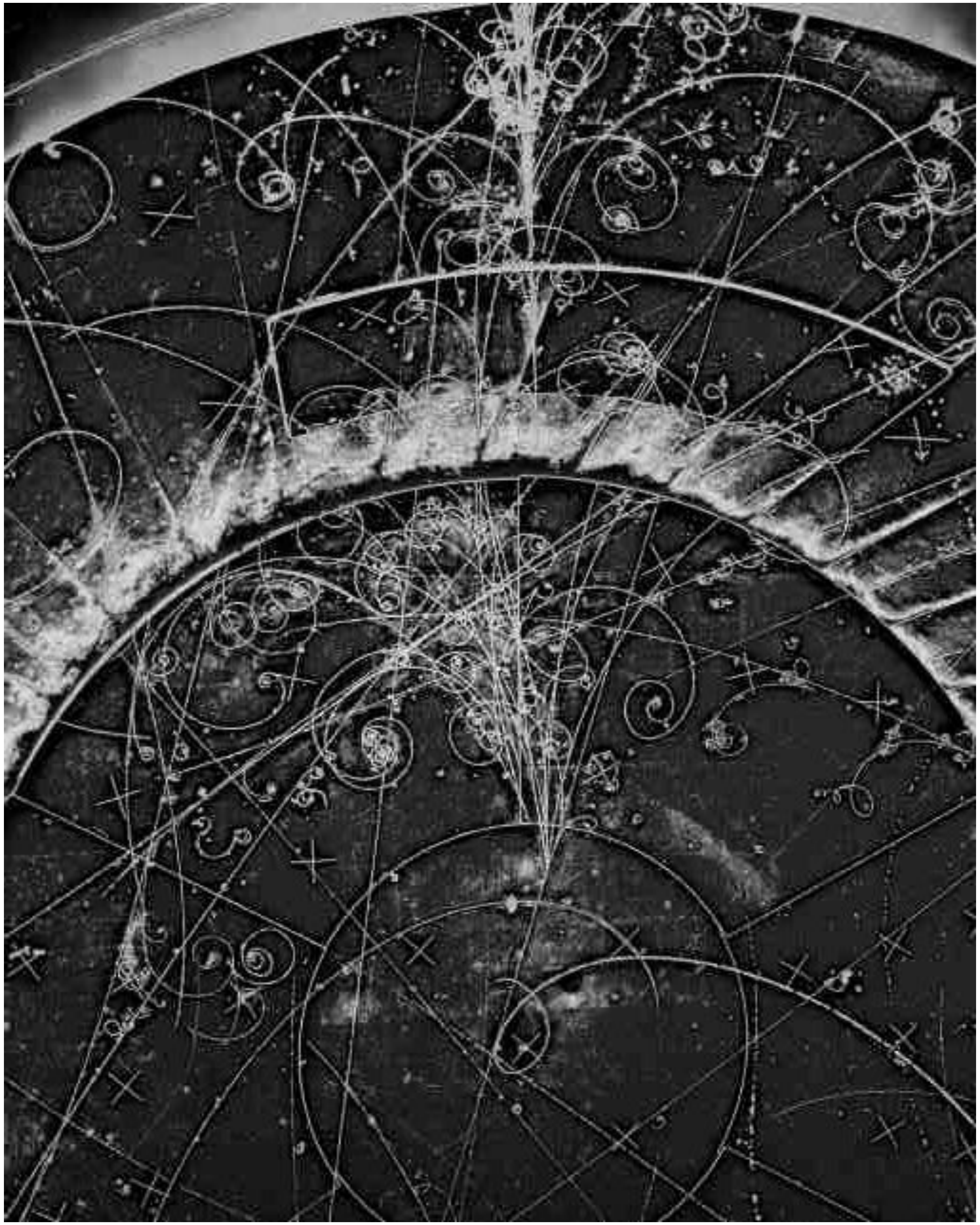

1 GeV/c π^- in una camera a bolle a idrogeno liquido

A) $\pi^- + p \rightarrow K^0 + \Lambda$

B) $K^0 \rightarrow \pi^- + \pi^+$

C) $\Lambda \rightarrow p + \pi^-$

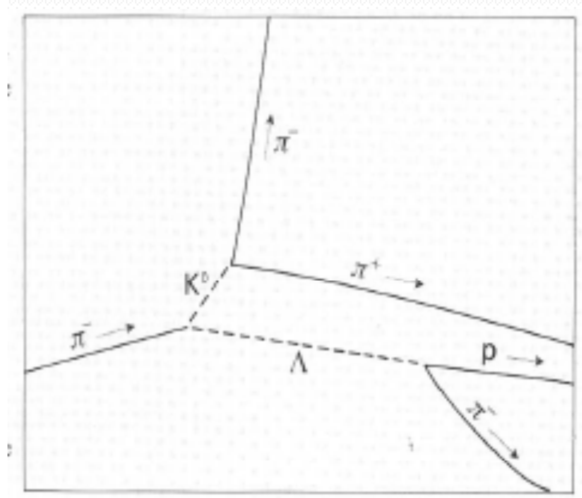

$particella$	$massa\ (MeV/c^2)$	$decadimento$	$vita\ media\ (s)$
$K^{\pm}$	494	$K^{\pm} \rightarrow \pi^{\pm}\pi^{0}$	$1.24\ 10^{-8}$
K^{0}	498	$K^{0} \rightarrow \pi^{-}\pi^{+}$	$0.89\ 10^{-10}$
Λ^{0}	1116	$\Lambda^{0} \rightarrow p\pi^{-}$	$2.63\ 10^{-10}$

$K^+p \rightarrow$	K^+p					
$K^+n \rightarrow$	K^+n	K^0p				
$K^-p \rightarrow$	K^-p	$\overline{K}^0 n$	$\pi^0\Lambda^0$	$\pi^+\Sigma^-$	$\pi^0\Sigma^0$	$\pi^-\Sigma^+$
$K^-p \rightarrow$	$K^0\Xi^0$	$K^+\Xi^-$				
$K^-n \rightarrow$	K^-n	$\pi^-\Lambda^0$	$\pi^0\Sigma^-$			
$K^-n \rightarrow$	$K^0\Xi^-$					

barione	*massa* (MeV/c^2)	*decadimento*	*vita media* (s)
Ξ^0	1315	$\Xi^0 \rightarrow \Lambda^0\pi^0$	$2.90\ 10^{-10}$
Ξ^-	1321	$\Xi^- \rightarrow \Lambda^0\pi^-$	$1.64\ 10^{-10}$

barioni $\frac{1}{2}^+$	A	S	Y	I_3	Q	*mesoni* 0^-	A	S	Y	I_3	Q
p	$+1$	0	$+1$	$+1/2$	$+1$	K^+	0	$+1$	$+1$	$+1/2$	$+1$
n	$+1$	0	$+1$	$-1/2$	0	K^0	0	$+1$	$+1$	$-1/2$	0
Λ^0	$+1$	-1	0	0	0	η^0	0	0	0	0	0
Σ^+	$+1$	-1	0	$+1$	$+1$	π^+	0	0	0	$+1$	$+1$
Σ^0	$+1$	-1	0	0	0	π^0	0	0	0	0	0
Σ^-	$+1$	-1	0	-1	-1	π^-	0	0	0	-1	-1
Ξ^0	$+1$	-2	-1	$+1/2$	0	$\bar{K}^0$	0	-1	-1	$+1/2$	0
Ξ^-	$+1$	-2	-1	$-1/2$	-1	K^-	0	-1	-1	$-1/2$	-1

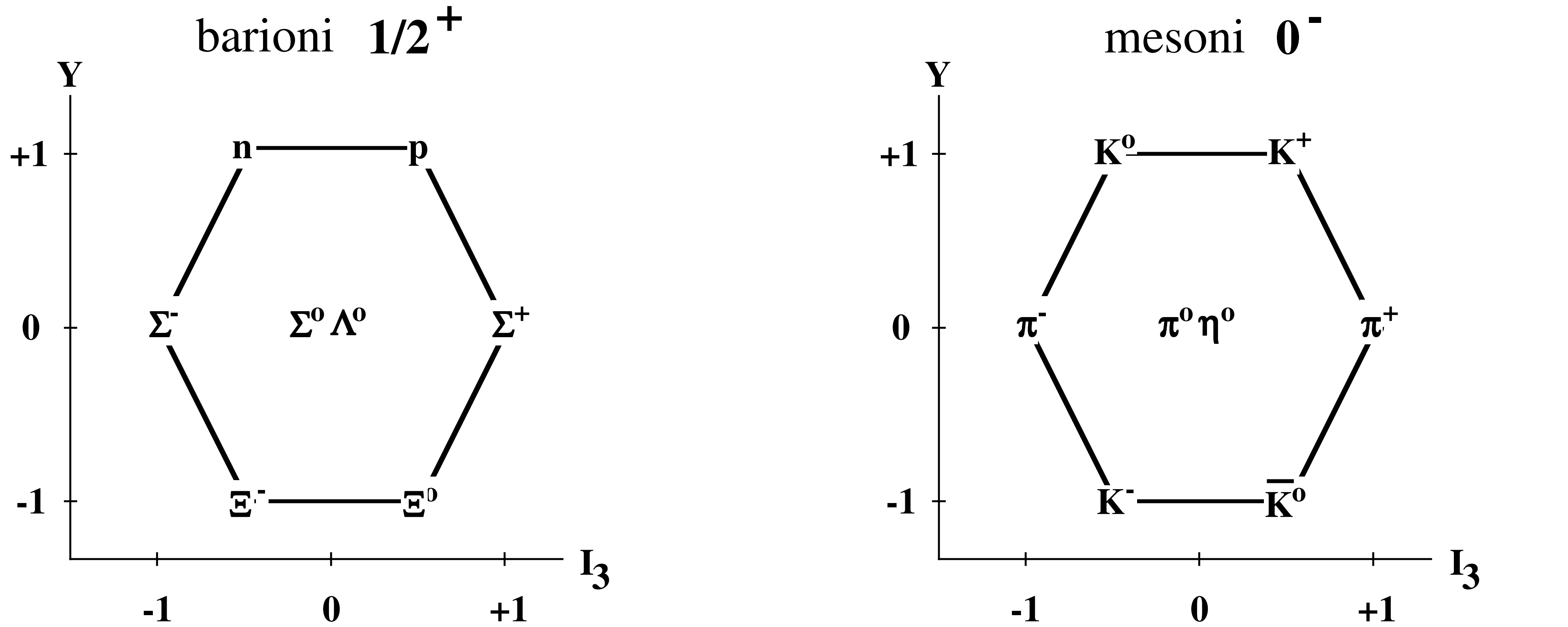

Figure 3.4: Rappresentazione degli stati dei barioni $\frac{1}{2}^+$ e dei mesoni 0^- nelle variabili $I_3 \times Y$

$\pi^0 \to \gamma\gamma$	0.988	*interazione elettromagnetica*
$\pi^0 \to e^+e^-\gamma$	0.012	$\tau = 0.84\ 10^{-16}\ s$
$\pi^0 \to e^+e^-$	$6.5\ 10^{-8}$	
$\pi^+ \to \mu^+\nu_\mu$	1.000	*interazione debole*
$\pi^+ \to e^+\nu_e$	$1.2\ 10^{-4}$	$\tau = 2.60\ 10^{-8}\ s$
$\pi^+ \to \pi^0 e^+\nu_e$	$1.0\ 10^{-8}$	

$K^+ \rightarrow$	$\mu^+\nu_\mu$	0.635	*decadimenti*
	$e^+\nu_e$	$1.6\ 10^{-5}$	*leptonici*
	$\pi^0 e^+\nu_e$	0.048	*decadimenti*
	$\pi^0\mu^+\nu_\mu$	0.032	*semileptonici*
	$\pi^+\pi^0$	0.212	*decadimenti*
	$\pi^+\pi^+\pi^-$	0.056	*adronici*
	$\pi^+\pi^0\pi^0$	0.017	

$\pi^0 \rightarrow \gamma\gamma$	0.988	*interazione elettromagnetica*
$\pi^0 \rightarrow e^+e^-\gamma$	0.012	$\tau = 0.84\ 10^{-16}\ s$
$\pi^0 \rightarrow e^+e^-$	$6.5\ 10^{-8}$	
$\pi^+ \rightarrow \mu^+\nu_\mu$	1.000	*interazione debole*
$\pi^+ \rightarrow e^+\nu_e$	$1.2\ 10^{-4}$	$\tau = 2.60\ 10^{-8}\ s$
$\pi^+ \rightarrow \pi^0 e^+\nu_e$	$1.0\ 10^{-8}$	